Tunable bandwidth optical rotator

Emiliya Dimova,[1] Andon Rangelov,[2,3,*] and Elica Kyoseva[3]

[1]*Institute of Solid State Physics, Bulgarian Academy of Sciences, 72 Tsarigradsko Chaussée, 1784 Sofia, Bulgaria*
[2]*Department of Physics, Sofia University, 5 James Bourchier Blvd., 1164 Sofia, Bulgaria*
[3]*Engineering Product Development, Singapore University of Technology and Design, 8 Somapah Road,*
487372 Singapore, Singapore
Corresponding author: rangelov@phys.uni-sofia.bg

We propose and experimentally demonstrate a novel type of polarization rotator that is capable of rotating the polarization plane of a linearly polarized light at any desired angle in either broad or narrow spectral bandwidth. The rotator comprises an array of standard half-wave plates rotated at specific angles with respect to their fast-polarization axes. The performance of the rotator depends on the number of individual half-wave plates, and in this paper we experimentally investigate the performance of two composite rotators comprising 6 and 10 half-wave plates.   © 2015 Chinese Laser Press

OCIS codes: (260.5430) Polarization; (260.1440) Birefringence; (260.2130) Ellipsometry and polarimetry.
http://dx.doi.org/10.1364/PRJ.3.000177

1. INTRODUCTION

Devices that rotate the polarization plane of a linearly polarized light at a selected angle are key elements of polarization state manipulation. Typically, these devices employ either the magneto-optic effect (i.e., Faraday rotator), the birefringent effect, or total internal reflection [1–5].

The Faraday rotator is made of a magnetoactive medium that is placed inside a strong magnet. The magnetic field induces different refraction indices for the left and right circularly polarized light, and as a result, the plane of linear polarization is rotated [1–5]. However, the angle of rotation is strongly dependent on the wavelength of the light. Similarly, the polarization rotation of birefringent base instruments is substantially wavelength dependent. In contrast, Fresnel rhombs, which are designed to use total internal reflection, can operate over a wide range of wavelengths but induce optical beam displacement in the lateral direction [1–5].

It is the object of the present paper to overcome the main disadvantages of current state-of-the-art polarization rotation devices and to provide an optical scheme for rotating the polarization plane of linearly polarized light that is relatively simple, flexible, inexpensive, and easily tunable to different rotation angles. Moreover, the device can be used in either broadband or narrowband regime. Here we report an experimental demonstration of such a device, which comprises a sequence of ordinary half-wave plates rotated at specific angles with respect to their fast-polarization axes. For the broadband regime, the design is assembled according to the recent theoretical work of Rangelov and Kyoseva [6].

2. THEORY

The Jones matrix for a retarder with a phase shift φ rotated at an angle θ is conveniently parameterized in the left–right circular polarization (LR) basis as

$$\mathbf{J}_\theta(\varphi) = \begin{bmatrix} \cos(\varphi/2) & i\,\sin(\varphi/2)e^{2i\theta} \\ i\,\sin(\varphi/2)e^{-2i\theta} & \cos(\varphi/2) \end{bmatrix}, \quad (1)$$

where half- and quarter-wave plates rotated at an angle θ are described by $\mathbf{J}_\theta(\pi)$ and $\mathbf{J}_\theta(\pi/2)$, respectively.

A sequence of N wave plates, each with a phase shift φ and rotated at an angle θ_k, then realizes the total Jones matrix

$$\mathbf{J}^{(N)} = \mathbf{J}_{\theta_N}(\varphi)\mathbf{J}_{\theta_{N-1}}(\varphi)\ldots\mathbf{J}_{\theta_1}(\varphi). \quad (2)$$

Our first goal is to design the sequence of half-wave plates such that the composite Jones matrix $\mathbf{J}^{(N)}$ from Eq. (2) produces a Jones matrix of a half-wave plate that is highly robust to variations in the phase shift φ around a selected value of φ. For the broadband composite half-wave plate we require a flat rotation profile around phase shift $\varphi = \pi$ [6], and for the narrowband composite half-wave plate we require a flat rotation profile around phase shift $\varphi = 2\pi$. We achieve this through the use of the control parameter θ_k. That is, we fix one of the N rotation angles θ_k such that the Jones matrix $\mathbf{J}^{(N)}$ from Eq. (2) is that of a half-wave plate. We use the other $N-1$ rotation angles to set the first $(N-1)/2$ nonvanishing derivatives of $\mathbf{J}^{(N)}$ with respect to the phase shift φ to zero at the desired value of φ, either for broadband (BB) or narrowband (NB):

$$\text{BB:}\ [\partial_\varphi^k \mathbf{J}^{(N)}]_{\varphi=\pi} = 0\left(k = 1, 2, \ldots, \frac{N-1}{2}\right), \quad (3a)$$

$$\text{NB:}\ [\partial_\varphi^k \mathbf{J}^{(N)}]_{\varphi=2\pi} = 0\left(k = 1, 2, \ldots, \frac{N-1}{2}\right). \quad (3b)$$

In such a manner we obtain a system of N coupled nonlinear algebraic equations for the N phases, which have multiple solutions for both broadband and narrowband conditions. Several solutions for the rotation angles θ_k of the individual half-wave plates for three and five composite sequences are shown in Table 1. The table shows sequences for broadband and narrowband half-wave plates, which we use for experimental realization of the polarization rotator.

Table 1.   Calculated Angles (in Degrees) of the Optical Axes of the Individual Half-Wave Plates to Implement Composite Sequences of Broadband and Narrowband Half-Wave Plates

Broadband Half-Wave Plates	
N	$(\theta_1; \theta_2; \ldots; \theta_N)$
3	(30; 150; 30)
5	(51.0; 79.7; 147.3; 79.7; 51.0)

Narrowband Half-Wave Plates	
N	$(\theta_1; \theta_2; \ldots; \theta_N)$
3	(150; 90; 30)
5	(137.0; 93.7; 158.2; 52.7; 31.2)

Then, for a given target polarization rotation angle α and a fixed number of half-wave plates N, one can find the exact values for the rotation angles θ_k in Table 2 of Ref. [6].

3. EXPERIMENT

Once we have the recipes for broadband and narrowband composite half-wave plates (cf. Table 1), we can experimentally construct the respective polarization rotators. It is well known [6,7] that two crossed half-wave plates realize a polarization rotator, where the angle between their fast axes is half the angle of polarization rotation. Here, we extend the idea further and utilize two crossed identical broadband or narrowband composite half-wave plates. In detail, we construct the polarization rotators as a sequence of two composite half-wave plates with angles θ_k from Table 1, which are crossed at an angle with respect to their fast axes. Such an arrangement rotates the polarization plane of a linearly polarized light at an angle equal to twice the angle between the optical axes of the composite half-wave plates. We use both broadband and narrowband composite half-wave plates as building blocks to realize broadband and narrowband polarization rotators, respectively.

We study the experimental properties of the composite rotators by analyzing the polarization of the transmitted light. The experimental setup, shown in Fig. 1, consists of three main parts: a source of polarized white light, a composite polarization rotator, and the light-analyzing part. A collimated beam of polarized light with a continuous spectrum was obtained using a 10 W halogen-bellaphot (Osram) lamp with a DC power supply, iris, two lenses, and a polarizer. The iris I imitates a point source of white nonpolarized light, which has been placed in the focus of the first lens L_1 ($f = 35$ mm) and additionally collimated by the second lens L_2 ($f = 150$ mm). The light beam formed is linearly polarized after passing through the

first polarizer P_1 [Glan-Taylor, 210–1100 nm, borrowed from a Lambda 950 spectrometer (Perkin Elmer)].

We used composite half-wave plates comprising $k = \{3, 5\}$ ordinary multi-order quarter-wave plates (WPMQ10M-780, Thorlabs), which perform as half-wave plates at $\lambda = 763$ nm. Each wave plate [aperture of 1 in. (0.0254 m)] was assembled onto a separate RSP1 rotation mount, which can realize a 360° rotation. The optical axes of all wave plates were determined with an accuracy of 1°. Each of them was rotated at the respective theoretically calculated angle θ_k (Table 1). Lastly, the wave plates were slightly tilted [8] to reduce unwanted reflections.

The analysis of the rotation effect of the composite polarization rotator was done by a system made up of an analyzer P_2 (same type as P_1), a plano–convex lens L_3 ($f = 20$ mm), and a two-axis micropositioner, which were used to focus the light beam onto the optical fiber entrance F connected to a grating monochromator (AvaSpec-3648 fiber-optic spectrometer with controlling software AvaSoft 7.5). With the available light source and monochromator, we obtained reliable spectral transmission data in the range of 400–1100 nm.

The measurement procedure was similar to the one described in Ref. [9]. We used a single beam spectrometer, and thus all experiments started with measurement of the dark and reference spectra. The dark spectrum, taken with the light path blocked, is further used to automatically correct for hardware offsets. The reference spectrum is usually taken with the light source on and using a blank sample rather than the sample under test. In our case, however, we measured the transmission spectrum of the already assembled composite polarization rotator, with the axes of the polarizer P_1 and the analyzer P_2 and the fast axis of the single wave plates all set to be parallel. The measured light spectrum was used as a reference for the subsequent measurements.

Finally, we assembled the two composite half-wave plates and rotated the first one at an angle $\alpha/4$ clockwise and the second one at an angle $\alpha/4$ counterclockwise. The analyzer P_2 was set to α with respect to P_1. The transmission spectrum of the realized composite polarization rotator was recorded and scaled to the reference spectrum. The unavoidable losses due to reflections and absorptions from any single wave plate were thereby taken into account.

We show the polarization rotation by the broadband and narrowband composite polarization rotators at four different rotation angles ($\alpha = 40°, 60°, 80°, 100°$) in Figs. 2 and 3, respectively. For easy reference and comparison of the broadband and narrowband behavior of the composite polarization rotators, we include the measured transmittance of a polarization rotator constructed of two ordinary half-wave plates.
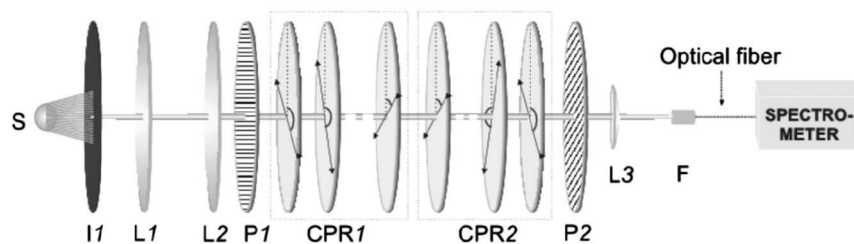

Fig. 1.   Experimental setup. The source S, iris I, lens L_1, lens L_2, and polarizer P_1 form a collimated beam of white polarized light. Polarizer P_2 and lens L_3 focus the beam of output light onto the entrance F of an optical fiber connected to a spectrometer. The two parts of the composite polarization rotator, which is constructed of a stack of multiple-order half-wave plates, are denoted as CPR1 and CPR2.
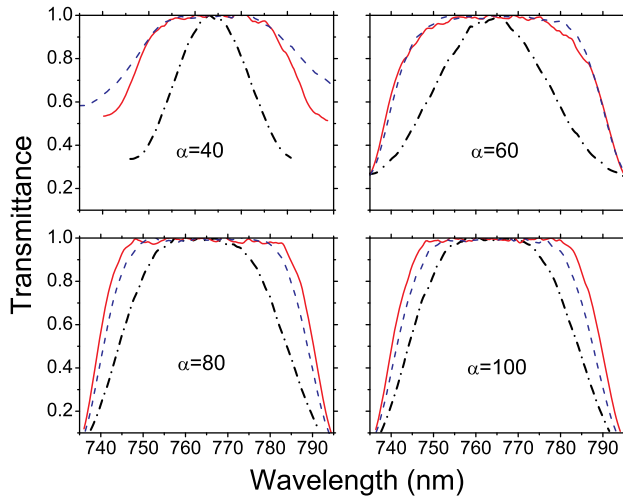
Fig. 2. Measured transmittance for two different composite broadband rotators. The blue dashed line represents a rotator with six half-wave plates, while the red solid line represents a rotator with 10 half-wave plates. The black dash-dotted line represents a rotator comprising two half-wave plates for easy reference.
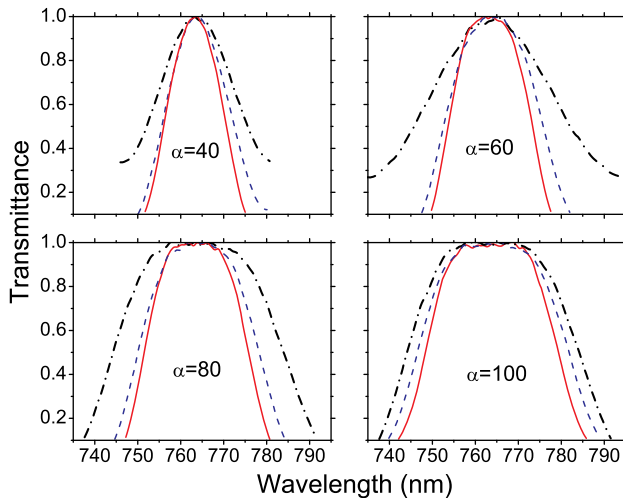

Fig. 3. Measured transmittance for two different composite narrowband rotators. The blue dashed line represents a rotator with six half-wave plates, while the red solid line represents a rotator with 10 half-wave plates. The black dash-dotted line represents a rotator comprising two half-wave plates for easy reference.

As predicted, we observe that the broadband and narrowband composite polarization rotators outperform the ordinary polarization rotator, and that the broadening and narrowing of the bandwidth increases with the number of half-wave plates in the sequence.

Next we turn our attention to the problem of misalignment of the orientation angles of the optic axis for each wave plate in the array, as such errors are always present in an experimental setup. In the case of broadband rotators, such errors are compensated automatically and do not affect the spectra visibly. We can show this by introducing additional misalignment and realizing that the overall results in Fig. 2 are not changed. However, for narrowband rotators the precise con-

trol of the orientation angles is more crucial, and therefore better control of the orientation angles leads to considerable improvement in the narrowing of our spectrum in Fig. 3.

4. CONCLUSION

In this paper, we demonstrated a novel, simple, multipurpose, and inexpensive composite polarization rotator that is capable of rotating the polarization plane of linearly polarized light at any desired angle. We showed that the bandwidth of the composite polarization rotator can be freely controlled by varying the number of constituent half-wave plates. Furthermore, we demonstrated that the constructed polarization rotator can be tuned to operate in both broadband and narrowband regimes by appropriately adjusting the rotation angles of each of the half-wave plates.

We note the universal principle that two crossed half-wave plates serve as a polarization rotator, and therefore any previously suggested achromatic half-wave plates [10–15] may be used to achieve a broadband polarization rotator.

REFERENCES

1. E. Hecht, *Optics* (Addison Wesley, 2002).
2. M. Born and E. Wolf, *Principles of Optics* (Cambridge University, 2005).
3. D. Goldstein and E. Collett, *Polarized Light* (Marcel Dekker, 2003).
4. M. A. Azzam and N. M. Bashara, *Ellipsometry and Polarized Light* (North Holland, 1977).
5. F. J. Duarte, *Tunable Laser Optics* (Elsevier Academic, 2003).
6. A. A. Rangelov and E. Kyoseva, "Broadband composite polarization rotator," Opt. Commun. **338**, 574–577 (2015).
7. J. S. Kim and J. K. Chang, "Achromatic polarization rotator and circular polarizer consisting of two wave plates of the same material," J. Korean Phys. Soc. **48**, 51–55 (2006).
8. T. Peters, S. S. Ivanov, D. Englisch, A. A. Rangelov, N. V. Vitanov, and T. Halfmann, "Variable ultrabroadband and narrowband composite polarization retarders," Appl. Opt. **51**, 7466–7474 (2012).
9. E. Dimova, S. S. Ivanov, G. Popkirov, and N. V. Vitanov, "Highly efficient broadband polarization retarders and tunable polarization filters made of composite stacks of ordinary wave plates," J. Opt. Soc. Am. A **31**, 952–956 (2014).
10. S. Pancharatnam, "Achromatic combinations of birefringent plates. Part I: an achromatic circular polarizer," Proc. Indian Acad. Sci. **41**, 130–136 (1955).
11. S. Pancharatnam, "Achromatic combinations of birefringent plates. Part II: an achromatic quarter-WP," Proc. Indian Acad. Sci. **41**, 137–144 (1955).
12. C. J. Koester, "Achromatic combinations of half-wave plates," J. Opt. Soc. Am. **49**, 405–409 (1959).
13. A. M. Title, "Improvement of birefringent filters. 2: achromatic waveplates," Appl. Opt. **14**, 229–237 (1975).
14. C. M. McIntyre and S. E. Harris, "Achromatic wave plates for the visible spectrum," J. Opt. Soc. Am. **58**, 1575–1580 (1968).
15. A. Ardavan, "Exploiting the Poincaré–Bloch symmetry to design high-fidelity broadband composite linear retarders," New J. Phys. **9**, 24 (2007).